31 October 2022

Vaisala RS41 Radiosondes Data Quality Report Sundowner Winds Experiment (SWEX 2022)

Holger Vömel, William Brown
Earth Observing Laboratory
National Center for Atmospheric Research
Boulder, CO

Earth Observing Laboratory
In situ Sensing Facility

National Center for Atmospheric Research
Boulder, Colorado

The Vaisala RS41 radiosonde data for this project were quality controlled and are maintained by the Earth Observing Laboratory at the National Center for Atmospheric Research (NCAR). The National Center for Atmospheric Research is managed by the University Corporation for Atmospheric Research and sponsored by the National Science Foundation.

If information or plots from this document are used for publication or presentation purposes, please provide appropriate acknowledgement to NCAR/EOL and NSF and refer to the citation listed below. Please feel free to contact the authors for further information.

Contacts:

Holger Vömel (voemel@ucar.edu)
Bill Brown (wbrown@ucar.edu)

Radiosonde operators:

NCAR: Brigitte Baeuerle, Liz Bernhardt, Bill Brown, Matt Paulus, Chris Roden, John Sobtzak, Isabel Suhr, Lara Tudor, Lou Verstraete, Jacquie Witte,

UCSB: Jean Allen, Silvana Castillo Guerra, Merissa Coello, Kristofer Daum, Sarah Ferguson, Janin Guzman-Morales, Devin Hernandez, Zhe Li, Ye Mu, Marian de Orla-Barile, Jordan Thomas, Kevin Varga, Em Waters

Mailing Address:

NCAR/Earth Observing Laboratory
P.O. Box 3000
3090 Center Green Dr.
Boulder, CO 80301, USA

Websites:

SWEX home page:
https://www.eol.ucar.edu/field_projects/swex
SWEX at U. Notre Dame:
https://efmlab.nd.edu/research/swex/
Integrated sounding system home page:
https://www.eol.ucar.edu/content/iss-operations-swex

To refer to the data sets or report, please include the following citations:

NCAR/EOL ISS Team, Geography Department, University of California, Santa Barbara. 2022. SWEX: ISS Radiosonde Data - Rancho Alegre Site. Version 1.0. UCAR/NCAR - Earth Observing Laboratory. https://doi.org/10.26023/J6P8-7SYD-XP0M. Accessed 03 Nov 2022.

NCAR/EOL ISS Team, Geography Department, University of California, Santa Barbara. 2022. SWEX: ISS Radiosonde Data - Sedgwick Site. Version 1.0. UCAR/NCAR - Earth Observing Laboratory. https://doi.org/10.26023/H5TV-Y54J-R010. Accessed 03 Nov 2022.

Document Version Control

Version	Date	Author	Change Description
1.0	31 Oct 2022	H. Vömel	Initial Data Release

1 Table of Contents

2 Dataset Overview

The Sundowner Winds Experiment (SWEX) studies the meteorological processes that control the downslope windstorms at the lee of the Santa Ynez Mountains in Santa Barbara County. These windstorms known as Sundowner winds are one of the most significant fire weather hazards affecting populated areas. They typically peak from early evening to mid-morning and modeling results show that the intensity and spatial variation of Sundowners are driven by a combination of dynamic and thermodynamic mechanisms that depend on the complex-terrain boundary layer dynamics, profiles of winds and stability.

The main goal of this study is to improve the current understanding of the dynamics and predictability of downslope windstorms in coastal Santa Barbara County. This project studies how the boundary layer structure and dynamics spanning the Santa Ynez Mountains and Santa Ynez Valley influence Sundowner winds intensity, timing and geographic characteristics. It examines mechanisms relating high amplitude mountain waves, critical layers, and surface wind intensity, and how variations in boundary layer structure and tropospheric stability influence the predictability of Sundowner winds.

Campaign staff from NCAR/EOL and the University of California, Santa Barbara (UCSB), successfully launched 187 Vaisala RS41 radiosondes at two sites, 88 at Sedgwick (ISS3) and 99 at Rancho Alegre (ISS2). Soundings were launched during Intensive Operations Periods (IOPs) as often as one sounding per 90 min. An overview of the number of soundings at each site is shown in Table 1.

Figure 1 shows the flight tracks of the ascending part of all soundings.

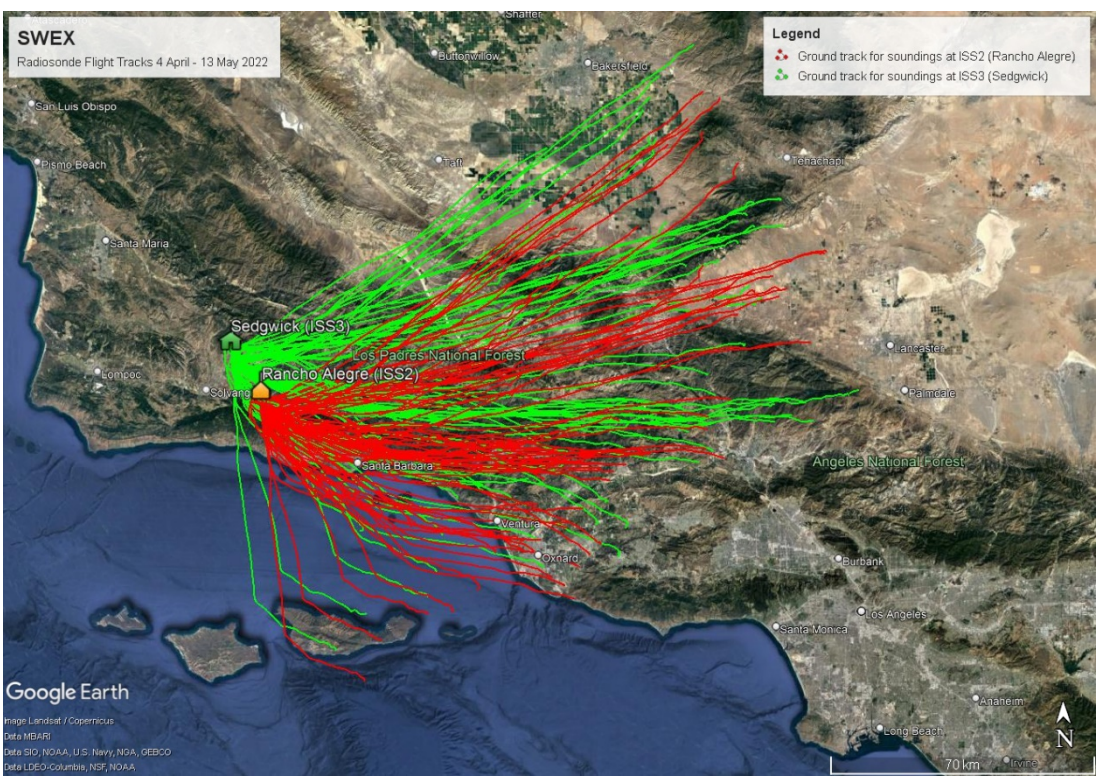

Figure 1: Location of the ISS2 and ISS3 sites during SWEX and flight tracks of all ascending radiosonde profiles. The sounding locations were 30 and 45 km north-west of Santa Barbara, CA.

Table 1: Number of soundings launched at each site

Date	IOP	Soundings Rancho Alegre	Soundings Sedgwick Reserve
Test soundings		2	1
05 Apr 2022	IOP1	8	8
13 Apr 2022	IOP2	4	1
14 Apr 2022	IOP3	8	7
18 Apr 2022	EOP1	8	8
23 Apr 2022	IOP4	6	8
25 Apr 2022	IOP5	8	8
26 Apr 2022	EOP2	8	7
29 Apr 2022	IOP6	8	8
05 May 2022	EOP3	10	10
08 May 2022	IOP7	3	3
09 May 2022	IOP8	10	10
11 May 2022	IOP9	9	9
13 May 2022	IOP10	7	0

3 Radiosonde sounding system

This campaign used Vaisala RS41-SGP radiosondes, which were received and processed by the Vaisala MW41 sounding system using software version 2.17.0. The radiosondes used by NCAR/EOL include a pressure sensor, which provides a better altitude and pressure determination in the boundary layer and is more suitable for unstable conditions in convective environments. The sounding system was configured to meet the needs of NCAR for high-resolution data and complete metadata description. All sondes were launched using 100 g balloons supplied by Scientific Sales.

The MWX raw data files from the sounding system were saved along with the ASCII output files, which contained the initially processed profiles.

Data were recorded also on descent; however, these data are not analyzed but can be made available only upon request.

The sounding systems automatically ingest surface reference observations, which are provided by sets of reference sensors near each launch site. These observations are stored in the surface observations metadata fields of the sounding files and used in the quality control procedures of the sounding data.

The reference sensors used for the radiosonde system during SWEX are listed in Table 2.

Table 2: Surface reference observations provided by the ISS meteorological reference sensors during SWEX.

Parameter	Location	Sensor
Pressure	The reference pressure was installed on a mast at 2 m height near the launch site.	PTB210
Temperature and humidity	The reference sensors for temperature and humidity were installed on a mast at 2 m height near the launch site.	Lufft WS300
Wind	The reference sensor for wind speed and wind direction was installed on a mast at 10 m height near the launch site.	Gill Wind Observer (2D sonic)

4 Quality control procedures

4.1 Standard quality control

The Vaisala system performs a sequence of standard quality control procedures and corrections for all radiosonde data:

- Applies a ground check correction for pressure using the pressure correction measured during the sonde preparation to compensate for small biases inherent in this type of pressure sensor.
- Performs a coarse outlier check for all measurement parameters
- Automatically detects launch based on change in pressure
- Performs a radiation correction for the temperature measurement using the radiation correction lookup table for the Vaisala RS41 radiosonde
- Corrects for response time lag of the temperature sensor
- Smooths the temperature profile
- Corrects for response time lag of the humidity sensor
- Filters out the balloon pendulum effect in the calculation of winds
- Calculates geopotential altitude based on the measured pressure profile

4.2 Custom quality control

In addition to the standard Vaisala procedures, all metadata are verified, and all measured parameters including reference measurements are checked for consistency and for any previously unidentified issue. The radiosonde measurements before launch are compared against the reference measurements and the causes for early termination are investigated. In the SWEX data set, the following issues were identified and corrected:

a. One sounding (ISS2, 20220405_230010) encountered a very strong downdraft and stopped real time processing. The missing data were restored from the raw data recording, which continued after the downdraft.

b. The reference wind sensor at Rancho Alegre, ISS2, relied on an incorrect configuration that caused all surface reference winds to be rotated by 180°. The Vaisala system makes use of the surface reference wind in the smoothing of the balloon borne wind profile near the surface. As a result, the wind direction measured by the balloons in the lowest 100 m is incorrect. This error was corrected in post-processing using the raw balloon wind measurements and the corrected surface reference winds.

c. The elevation of the launch location at Rancho Alegre, ISS2, was at an altitude 3 m higher than configured in the sounding system. The launch elevation and reference pressure, which are given in the first data line of the final data set, were adjusted accordingly.

d. In a small number of soundings, the time at which launch was detected was adjusted by up to two seconds to improve the resolution of observations near the surface.

e. The vertical wind speed was calculated as the difference between the measurement balloon rise rate and a theoretical balloon ascent rate. This theoretical balloon ascent rate was taken as the average ascent rate of all balloons. All soundings used the same sonde and balloon type and the amount if gas was controlled to within 10% for all balloons (see discussion below) allowing the use of the average ascent rate as the expected value.

4.3 Data format

The final quality-controlled data are provided in NetCDF format following the CF-1.6 metadata convention for climate and forecasting. For a detailed description of the data format, refer to Vömel et al. (2018), https://doi.org/10.5065/D65X27SR.

5 Sounding metrics

NCAR launched radiosondes during SWEX at two sites. The ISS2 site was located at Rancho Alegre near lake Cachuma approximately 30 km NW of Santa Barbara. The ISS3 site was located at the Sedgwick Reserve, which is administered by the University of California, Santa Barbara, and located about 45 km NW of Santa Barbara. 99 balloons were launched at Rancho Alegre (ISS2) and 88 at Sedgwick Reserve (ISS3). Up to eight soundings per day were launched during Intensive Observation Periods (IOPs) with a spacing as close as every 90 min.

The distribution of ceiling heights is shown in Figure 2. Ceiling heights below 16 km were mostly due to early loss of telemetry signal. This occurred mostly in soundings launched at Rancho Alegre (ISS2), where the local topography near the launch site limited the line of sight for balloons that travelled particularly far east. All balloons ascended at the nominal rise rate and no sounding reported a failed sensor.

The balloon of sounding 20220419_105925 at Sedgwick Reserve (ISS3) burst 450 m above ground. Although very limited in altitude, the profile remains in the data set. Due to air traffic control limitations, a second balloon could not be launched at this location.

Data were received up to a distance of 164 km. The distribution of balloon distances at ceiling altitude and at 1 km above ground is shown in Figure 4. The median distance at which a sounding was terminated was 88 km for ISS2 and 111 km for ISS3. At 1 km above ground, the median distance was about 1.1 km from the launch site.

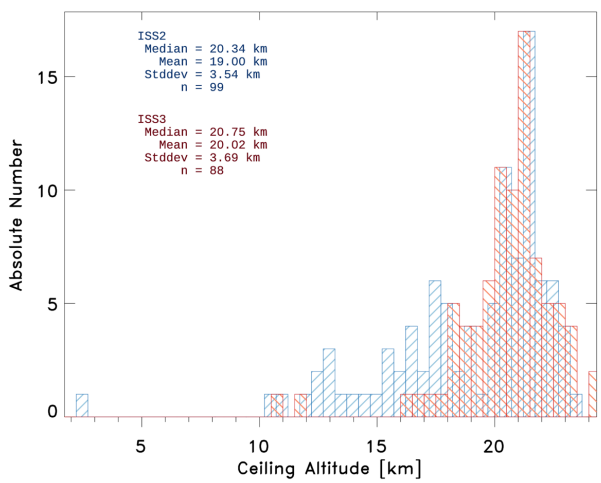

Figure 2: Distribution of ceiling heights for all radiosondes launched during SWEX. Data for ISS2 (Rancho Alegre) are shown in blue, those for ISS3 (Sedgwick Reserve) in red.

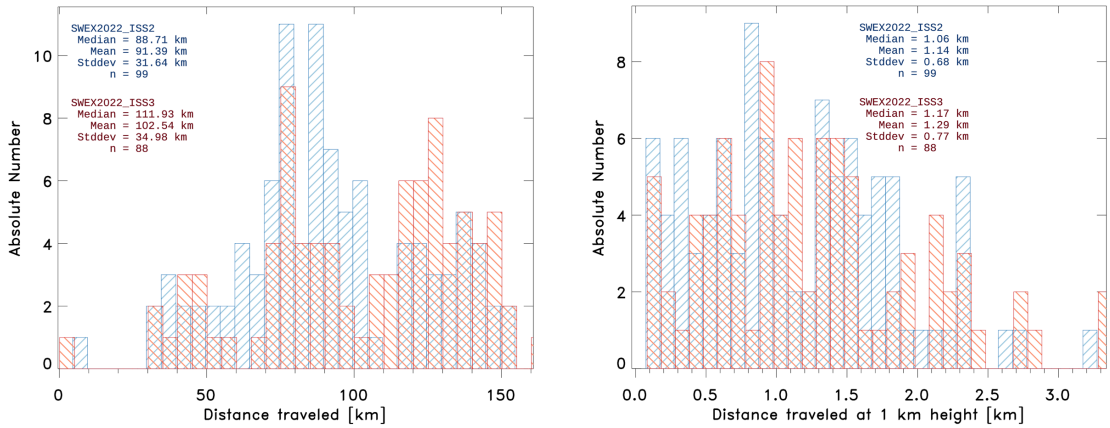

Figure 4: Distribution of balloon distance at end of data recording (left panel) and at 1 km above ground (right panel).

Balloons were nominally filled with 20 ft^3 of helium with a range from 20 to 24 ft^3. The rise rate difference between these fill amounts during SWEX is small. Balloons typically rose with between 3.5 m/s to 5.0 m/s. The profiles of the average rise rate for the two different fill volumes is shown in Figure 3. Balloons rose faster in the lowest 2 km with an average rise rate of about 4.5 m/s shortly after launch and a minimum of 3.5 m/s at about 4 km altitude. As a result, the vertical resolution of measurements in the lowest troposphere increases from about 4.5 m to 3.5 m between the surface 3 km altitude.

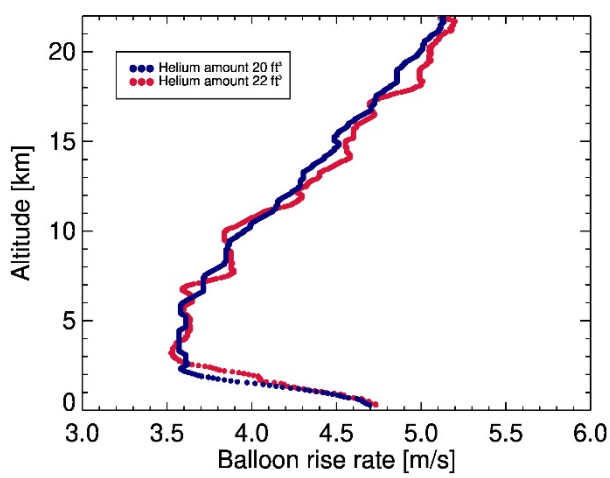

Figure 3: Average rise rates profiles for the different helium fill values used during SWEX.

The maximum rise rate over a 50 m layer was 10.5 m/s in sounding 20220509_080004 at Rancho Alegre (ISS2) observed in a shallow updraft. With few exceptions, all strong up and downdrafts were observed at Rancho Alegre (ISS2), which lies at the foot of the Santa Ynez Range. Five soundings at that site had layers of descending balloon motion and are listed in Table 3. Sounding 20220405_230010 at Rancho Alegre showed with 165 m the largest descent which triggered a premature termination by the Vaisala system. The trajectory of this sounding is shown in Figure 5.

Table 3: Soundings with periods of balloon descent

Sounding	Altitude drop [m]
ISS2_20220405_105959	-26
ISS2_20220405_140002	-23
ISS2_20220405_230010	-165
ISS2_20220508_033431	-4
ISS2_20220509_050306	-6

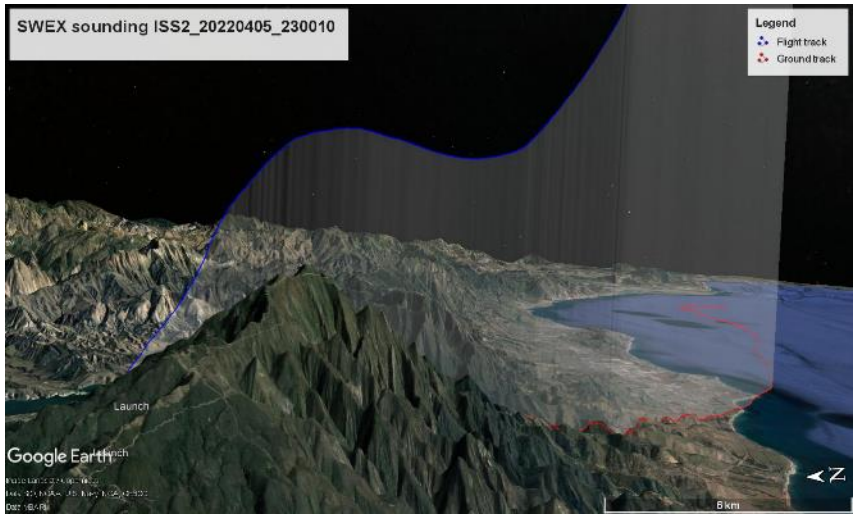

Figure 5: Trajectory for sounding 20220405_230010 at Rancho Alegre showing a region of descent.

The distribution of rise rates for all soundings is shown in Figure 5. The median of the balloon rise rates is identical at both sites; however, the distribution of rise rates is substantially wider at Rancho Alegre (ISS2), which is most likely related to the stronger updrafts in the vicinity of the mountain range. The balloon inflation is less likely responsible for this spread, since the amount of gas used at Rancho Alegre was more consistent than at Sedgwick Reserve.

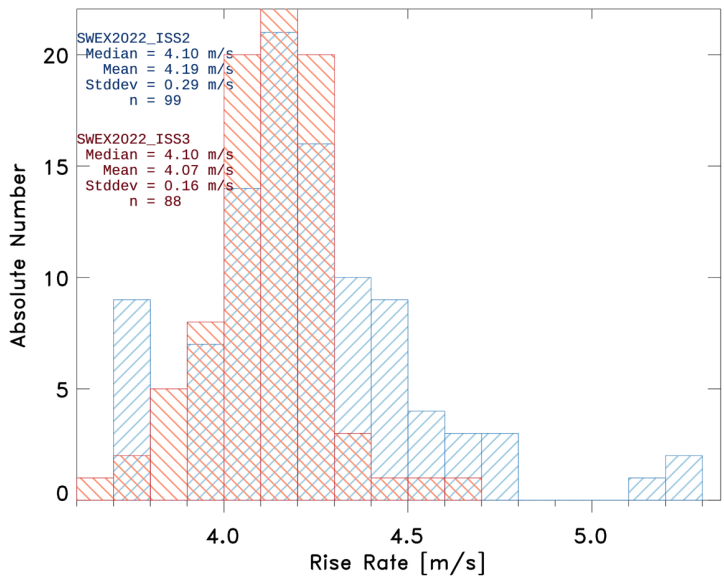

Figure 6: Distribution of rise rates for all radiosondes launched during SWEX.

The rise rates of all soundings are shown as sequential contour plot in Figure 7. Note that many more soundings at Rancho Alegre (ISS2, left plot) show large rise rate variations in the lowest 7 km compared to Sedgewick Reserve (ISS3, right plot), related to the different spread shown above.

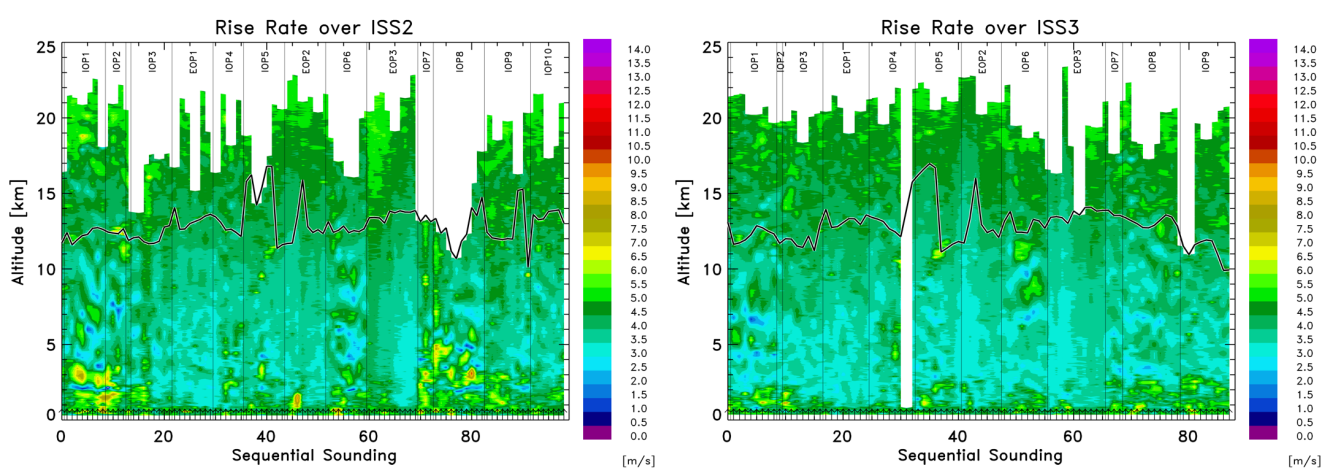

Figure 7: Sequential rise rate profiles as color contours for all radiosondes launched during SWEX. Left: Soundings at Rancho Alegre (ISS2). Right: Soundings at Sedgwick Reserve (ISS3). Each launch is indicated by a small arrow at the bottom of the diagram. The black line indicates the tropopause.

6 Atmospheric Measurements

Air temperature from all soundings are shown in Figure 8. Individual balloon launches in this and all following figures are indicated by arrows at the bottom of each panel. The intensive observation periods are separated by vertical lines and provide some indication when these soundings took place. Note that at Sedgwick Reserve (ISS3) fewer soundings were launched than at Rancho Alegre (ISS2).

Surface temperatures were above freezing for all soundings during the entire campaign. The tropopause (shown as thin black line) ranged typically between 13 and 15 km with extremes from 11 to 18 km.

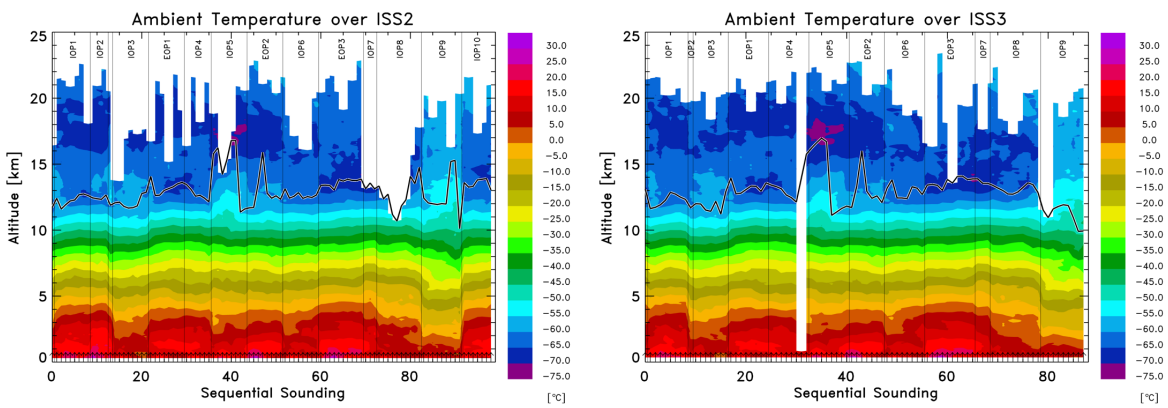

Figure 8: Sequential contours of temperature profiles at Rancho Alegre (ISS2, left) and at Sedgwick Reserve (ISS3, right) from all radiosondes launched during SWEX. The tropopause is shown as thin black line typically between 10 and 13 km.

Relative humidity from all soundings is shown in Figure 9. Relative humidity at altitudes above the freezing level is shown as relative humidity over ice to highlight the possibility for cirrus and mixed phase clouds. All relative humidity profiles are clipped at 100 % relative humidity over liquid. The tropopause marks the transition from the moist troposphere to the very dry stratosphere.

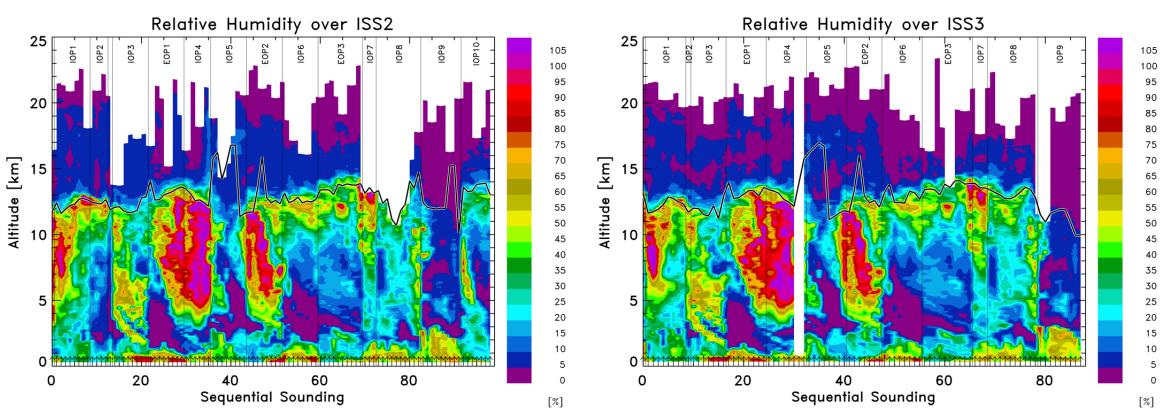

Figure 9: Sequential contours of relative humidity profiles at Rancho Alegre (ISS2, left) and at Sedgwick Reserve (ISS3, right) from all radiosondes launched during SWEX.

The zonal wind speed is shown in Figure 10. The jet stream stands out between IOP3 and IOP5 and again between IOP7 and IOP10.

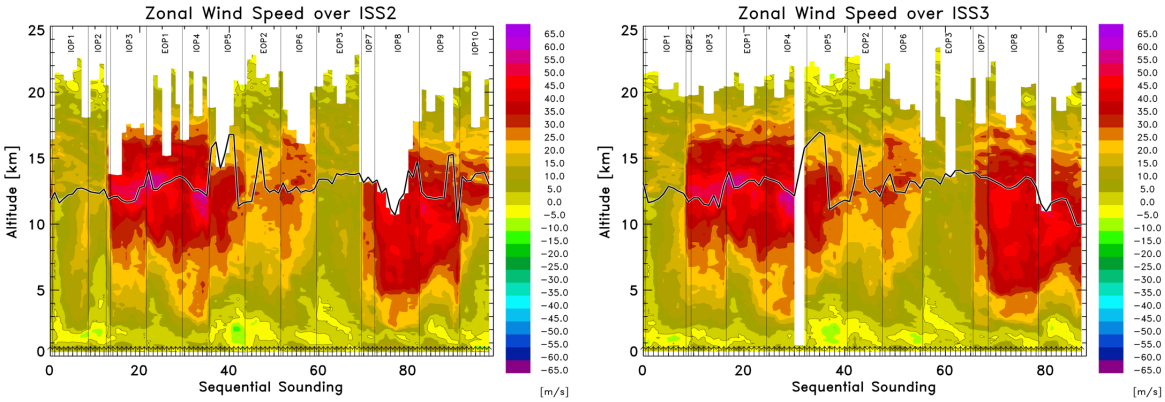

Figure 10: Sequential contours of zonal wind speed profiles at Rancho Alegre (ISS2, left) and at Sedgwick Reserve (ISS3, right) from all radiosondes launched during SWEX.

The meridional wind speed measurements are shown in Figure 11. The strongest meridional orientation of the jet stream was observed during IOP9. During IOP1 and IOP2 (4 to 6 April 2022) and again during EOP2 (25 to 26 April 2022), the stratospheric winds show a strong wave activity between 15 and 25 km. The strongest northerly winds in the lower troposphere were observed during IOP1 (4 to 5 April 2022)

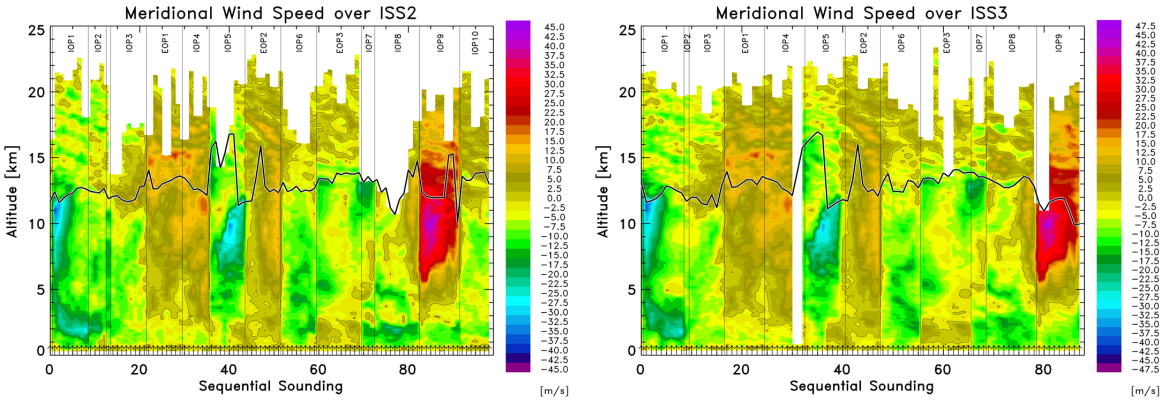

Figure 11: Sequential contours of meridional wind speed profiles at Rancho Alegre (ISS2, left) and at Sedgwick Reserve (ISS3, right) from all radiosondes launched during SWEX.

The vertical wind speed is derived from the difference between a theoretical and the actual balloon ascent speed (Wang et al., 2009) and shown in the Figure 12. The soundings at Rancho Alegre (ISS2, left) show a much stronger vertical winds and larger variability compared to the soundings at Sedgwick Reserve (ISS3, right). The uncertainty of this method is about 1m/s; updrafts stronger than 4 m/s below 6 km were observed at Rancho Alegre (ISS2) during IOP1 (4 April 2022) and IOP8 (8 May 2022).

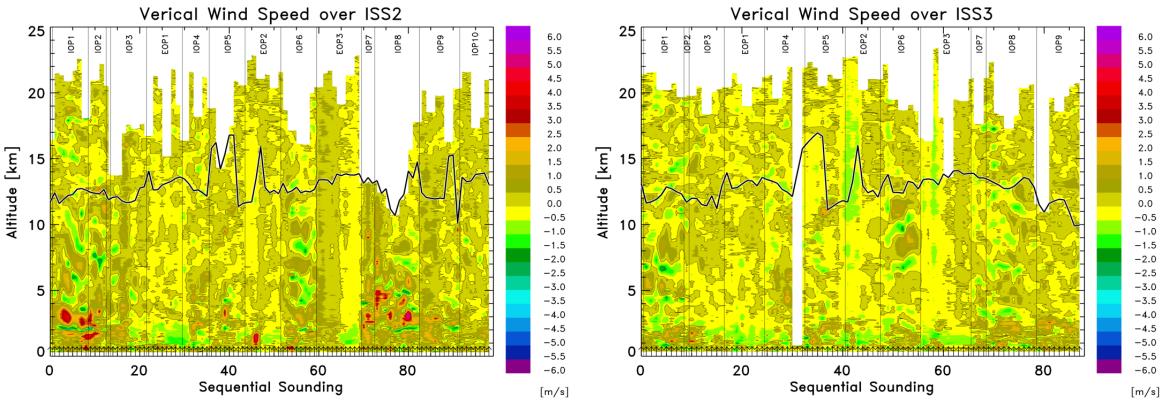

Figure 12: Sequential contours of vertical wind speed profiles at Rancho Alegre (ISS2, left) and at Sedgwick Reserve (ISS3, right) from all radiosondes launched during SWEX.

7 List of all soundings

7.1 Rancho Alegre (ISS2)

#	Date [UTC]	Time [UTC]	Radiosonde serial number	Ceiling altitude [km]	Rise rate [m/s]	Duration [min]
1	17-Mar-22	22:19:12	S0550986	16.4	4.3	62.8
2	4-Apr-22	17:00:07	S0551071	21.4	4.3	82.8
3	4-Apr-22	20:00:02	S0551014	21.6	4.4	80.3
4	4-Apr-22	23:00:03	S0551012	21.3	4.4	79.7
5	5-Apr-22	2:00:04	N2020249	20.9	4.3	79.3
6	5-Apr-22	5:00:02	S0551020	21.7	4.1	87.6
7	5-Apr-22	7:59:59	S0551009	22.7	4.1	91.4
8	5-Apr-22	10:59:59	S0551010	22.5	4.2	88.6
9	5-Apr-22	14:00:02	S0551019	18.1	4	74.4
10	5-Apr-22	23:00:10	S0551018	2.2	5.2	6.2
11	6-Apr-22	2:00:07	N2030141	20.9	4.3	80.2
12	6-Apr-22	5:00:02	S0550909	22.6	4.3	87.2
13	6-Apr-22	8:00:10	S0550890	22.1	4.2	87.1
14	9-Apr-22	23:02:19	S0550921	20.5	4.5	74.3
15	13-Apr-22	17:00:27	N2030218	13.8	3.8	58.7
16	13-Apr-22	20:00:08	N2020250	13.7	3.9	57.7
17	13-Apr-22	23:00:10	S0550922	16.9	4.7	58.6
18	14-Apr-22	2:00:03	S0550911	17.5	4.7	61.1
19	14-Apr-22	5:00:01	S0550912	18	3.8	76.8
20	14-Apr-22	8:00:00	S0551077	17.2	3.9	72.3
21	14-Apr-22	11:00:01	S0551079	17.6	4.1	70.5
22	14-Apr-22	14:00:01	S0551075	18.9	4.2	73.7
23	17-Apr-22	17:00:14	S0550889	16.7	4	68
24	17-Apr-22	20:00:14	N2030144	22.5	4	92.2
25	17-Apr-22	23:00:14	N2020248	21.2	4.1	85.7
26	18-Apr-22	2:00:14	N2020258	20.3	4.1	81.4
27	18-Apr-22	5:00:01	N2020265	15.2	3.7	66.4
28	18-Apr-22	8:00:00	S0550910	22.1	4.2	87.4
29	18-Apr-22	11:00:01	S0550920	21.7	4.1	88.1
30	18-Apr-22	14:00:00	S0550908	19	3.8	81.6
31	18-Apr-22	17:00:15	N2030143	16.4	3.7	73.1
32	18-Apr-22	20:00:14	N2030142	21.8	4.2	84.6
33	18-Apr-22	23:00:15	N2020247	21.6	4.4	80.5
34	19-Apr-22	2:00:14	N2020252	18.2	4	73.8
35	19-Apr-22	5:00:01	S0551098	21.8	4.2	85.9
36	19-Apr-22	8:00:03	S0551076	21.2	4.1	84.5
37	23-Apr-22	17:00:14	N2020256	18.8	4.2	73.1
38	23-Apr-22	20:00:11	S0551078	19.9	4.2	77.7
39	23-Apr-22	23:00:12	N2020267	14.3	4	58.4
40	24-Apr-22	2:00:11	N2020254	15.3	4.1	61.2
41	24-Apr-22	5:08:34	S0550893	17.5	4	71.7
42	24-Apr-22	8:00:01	S0550907	21.1	4.2	83.6
43	24-Apr-22	11:08:38	S0550923	20.9	4.1	83.2
44	24-Apr-22	14:00:00	S0540710	20.6	4.1	81.7
45	25-Apr-22	17:00:14	N2020266	22.4	4	92.2
46	25-Apr-22	20:00:12	N2030219	23.2	4.2	90.4
47	25-Apr-22	23:00:10	N2020268	22.8	4.1	90.6
48	26-Apr-22	2:00:12	S0540121	21	4.4	79
49	26-Apr-22	5:05:33	S0540166	21.7	4.2	85.4

50	26-Apr-22	8:00:01	S0540167	21.3	4.1	86
51	26-Apr-22	11:00:02	S0540678	20.4	4.1	80.9
52	26-Apr-22	14:00:02	S0540719	21.8	4	89.1
53	28-Apr-22	17:00:08	S0540164	21.6	4.3	83.5
54	28-Apr-22	20:00:24	S0540705	18.7	4.3	70.5
55	28-Apr-22	23:00:04	S0550924	17.1	4.1	68.7
56	29-Apr-22	0:30:00	S0540163	17.5	4.1	69.7
57	29-Apr-22	2:00:02	S0540677	16.1	3.7	71.1
58	29-Apr-22	3:30:02	S0530725	16	3.7	70.3
59	29-Apr-22	5:12:32	S0530679	19.9	4.1	80.5
60	29-Apr-22	8:00:02	S0530721	21.4	4	87.4
61	4-May-22	17:00:02	S0530716	20.4	4.7	71.4
62	4-May-22	18:36:20	S0530685	21.5	4.6	76
63	4-May-22	20:02:05	S0550424	22.3	4.5	80.9
64	4-May-22	23:00:09	S0530680	21.7	4.4	80.2
65	5-May-22	2:00:17	S0641815	20.5	4.4	75.8
66	5-May-22	3:30:02	S0530722	19.1	3.9	79.5
67	5-May-22	5:00:10	S0641816	21.3	4.1	86.2
68	5-May-22	8:00:02	S0530715	21.3	4	88.6
69	5-May-22	11:00:02	S0530684	22.8	3.9	95.9
70	5-May-22	14:15:54	S0530726	22.9	4.1	92.5
71	7-May-22	23:00:16	S0530683	13.1	4.1	52.1
72	8-May-22	1:59:40	S0530682	19.8	5.1	64.2
73	8-May-22	3:34:31	S0550421	13.2	4	54.1
74	8-May-22	17:00:09	S0550423	15.6	5.2	49.5
75	8-May-22	20:00:03	S0550444	12.4	4.4	45.8
76	8-May-22	23:00:08	S0550520	12.7	4.1	50.6
77	9-May-22	0:30:07	S0550521	11.2	4.2	43.5
78	9-May-22	2:00:03	S0530521	10.7	3.8	45.1
79	9-May-22	3:30:08	S0641900	11.8	3.9	49.3
80	9-May-22	5:03:06	S0641813	12.3	3.9	51.9
81	9-May-22	8:00:04	S0530520	15.7	4	63.4
82	9-May-22	11:00:00	S0641814	19.4	4	80.1
83	9-May-22	14:00:01	S0641858	17.8	3.9	73.8
84	10-May-22	17:00:28	S0641852	20.6	4.5	74.9
85	10-May-22	20:00:23	S0530519	20.2	4.6	71.5
86	10-May-22	23:01:00	S0530529	18.5	4.5	67.2
87	11-May-22	2:00:09	S0641899	20.3	4.6	73.1
88	11-May-22	3:30:24	S0530531	19.8	4.3	75.2
89	11-May-22	5:02:52	S0530534	20.7	4.1	83.8
90	11-May-22	8:00:01	S0530523	16.3	4.2	63.5
91	11-May-22	11:00:17	S0530518	20.6	3.8	89.4
92	11-May-22	14:00:17	S0530533	20.3	4.2	78.7
93	12-May-22	23:00:11	S0530546	23.6	4.3	91
94	13-May-22	2:00:01	S0530544	21.6	4.4	79.8
95	13-May-22	5:00:02	S0530539	21.7	4.2	84.2
96	13-May-22	7:59:59	S0530526	17.3	4.2	68.2
97	13-May-22	9:30:01	P0950467	18.1	4	73.5
98	13-May-22	11:00:01	P0950489	21	4.4	78.7
99	13-May-22	14:00:01	S0530545	21.5	4.3	81.6

7.2 Sedgwick Reserve (ISS3)

#	Date [UTC]	Time [UTC]	Radiosonde serial number	Ceiling altitude [km]	Rise rate [m/s]	Duration [min]
1	31-Mar-22	22:19:02	P5010548	21.4	4.2	84.2
2	4-Apr-22	17:00:12	T3320458	21.5	4.2	84.5
3	4-Apr-22	19:59:49	T3321884	22.3	4.2	87.6
4	4-Apr-22	22:59:51	T3321882	21.6	3.8	93.2
5	5-Apr-22	2:04:43	T3330428	20.2	3.9	84.8
6	5-Apr-22	5:01:12	S0551013	20.2	3.9	84.1
7	5-Apr-22	8:00:01	P5010547	20.7	4.1	82.8
8	5-Apr-22	10:59:39	T3330070	21	4.1	84.3
9	5-Apr-22	13:59:27	T3330267	19.7	4	81.2
10	13-Apr-22	16:59:59	T3340587	20.5	4	83.5
11	13-Apr-22	20:00:10	T3321879	19.8	4.2	77
12	13-Apr-22	22:59:08	T3321877	21.2	4.2	82.2
13	14-Apr-22	1:59:57	T3321890	20.5	4.1	81.3
14	14-Apr-22	5:00:06	P5010583	18.3	4	75.5
15	14-Apr-22	8:00:08	P5010599	20.1	4.1	79.5
16	14-Apr-22	11:00:21	R1740021	20.3	4.1	80.9
17	14-Apr-22	14:00:20	R1820183	21.3	4.2	84.1
18	17-Apr-22	17:00:19	P5010549	20.4	4	83.1
19	17-Apr-22	20:00:38	P5010564	21.6	4.1	86.8
20	17-Apr-22	23:00:39	N1620189	21.4	3.8	91.9
21	18-Apr-22	2:00:17	N1740098	20.6	4	84.7
22	18-Apr-22	5:00:37	P5010600	18.9	4	77.8
23	18-Apr-22	8:00:13	P5010579	20.8	4	85
24	18-Apr-22	11:00:09	P5010563	20.4	4.2	80.1
25	18-Apr-22	14:00:06	P5010550	21.2	4.1	85
26	18-Apr-22	17:00:15	P0950435	21.3	3.9	90.1
27	18-Apr-22	20:00:05	P0950410	23.4	4.1	94.4
28	18-Apr-22	23:00:35	P0950407	19.5	4.2	76.3
29	19-Apr-22	2:00:25	P0950434	20.9	4.1	83.4
30	19-Apr-22	4:59:59	P0950412	22.3	4.2	86.5
31	19-Apr-22	8:00:07	P0950436	22	4.5	80.5
32	19-Apr-22	10:59:25	P1140660	0.8	4.6	1.7
33	23-Apr-22	16:59:59	P0950318	21.9	4	90.7
34	23-Apr-22	20:00:02	P0950446	22.3	4	91.2
35	23-Apr-22	22:59:59	P0950406	22.7	4.1	90
36	24-Apr-22	2:00:04	N1740175	21.9	4	89.4
37	24-Apr-22	5:00:41	P1220151	20.5	4.1	81.2
38	24-Apr-22	8:01:22	N1740101	21.3	4	87.1
39	24-Apr-22	11:00:11	P1140657	21.8	4.2	85.3
40	24-Apr-22	14:00:17	P1220152	21	4.2	82.9
41	25-Apr-22	16:59:59	N4340792	23.4	3.9	98.5
42	25-Apr-22	20:00:06	N4340857	22.7	3.7	100.3
43	25-Apr-22	23:00:05	N4340854	23	3.9	97.7
44	26-Apr-22	2:00:07	N4340848	22.7	3.8	99.5
45	26-Apr-22	5:00:08	N4340868	20.2	4.1	81.6
46	26-Apr-22	8:00:09	N4350822	21	4.1	85
47	26-Apr-22	11:00:06	N4340864	21	4.1	83.5
48	26-Apr-22	14:00:03	N4340791	21	4.1	83.7
49	28-Apr-22	17:00:02	N4340585	22.2	4.1	87.9
50	28-Apr-22	20:00:03	N4340873	23.2	3.9	98.5
51	28-Apr-22	23:00:08	N4340866	19.4	4.1	78.1

52	29-Apr-22	0:30:03	N4340870	19.6	4.2	76.2
53	29-Apr-22	2:00:05	N4340865	18.7	4	76
54	29-Apr-22	3:30:01	N4340697	19	4.1	75.9
55	29-Apr-22	5:00:00	N4340849	21.2	4.2	82.2
56	29-Apr-22	8:00:00	N4340855	18.6	4.1	74.5
57	4-May-22	17:00:01	N4340586	16.5	3.6	75.5
58	4-May-22	18:30:14	N4410027	16.3	3.8	69.9
59	4-May-22	20:00:03	N4340847	23.3	3.7	103.4
60	4-May-22	23:00:07	N4340861	24.1	4	98.8
61	5-May-22	2:00:10	N4340860	18.1	3.9	76
62	5-May-22	3:30:02	N4330885	13.6	3.8	58
63	5-May-22	6:13:58	N4340581	20.7	4.1	83.8
64	5-May-22	8:00:55	N4340851	19.4	4.2	75.4
65	5-May-22	11:00:07	N4330884	19.4	4.1	76.9
66	5-May-22	14:00:08	N4340396	21	4.2	82.5
67	7-May-22	23:00:03	N4330883	22.7	4	93.5
68	8-May-22	2:00:14	N4340863	17.6	4.1	70.3
69	8-May-22	3:32:53	N4340884	21.1	4.1	83.6
70	8-May-22	17:00:11	N4340698	22.3	4	91.3
71	8-May-22	20:00:13	N4410029	24.3	4	100.2
72	8-May-22	23:00:21	N4410034	18.4	4	74.6
73	9-May-22	0:30:16	N4330886	18.2	4	75
74	9-May-22	2:00:18	N4340852	17.2	4	70.4
75	9-May-22	3:30:08	N4340862	18.2	4	74.2
76	9-May-22	5:00:12	N4340886	21.1	4.2	82.1
77	9-May-22	8:00:08	N4340856	20.4	4.3	78
78	9-May-22	11:00:07	N4410035	20.6	4.1	81.8
79	9-May-22	14:00:08	N4350395	20.7	4.3	78.9
80	10-May-22	17:00:22	N4340699	11.5	3.9	47.7
81	10-May-22	20:00:19	P0950480	10.9	4.1	43
82	10-May-22	23:00:15	P0950488	21.4	4.4	80.4
83	11-May-22	2:00:07	P0950479	19.6	4.2	77.1
84	11-May-22	3:30:12	P0950468	18.6	4.1	74
85	11-May-22	5:00:07	P0950478	19.7	4.2	76.6
86	11-May-22	8:00:04	P0950490	20.4	4.2	79.2
87	11-May-22	11:00:09	P0950491	20.7	4.3	79.4
88	11-May-22	14:00:09	P0950473	21	4.2	81.3

8 References

Vömel, H., G. Granger, and I. Suhr (2018): NCAR/EOL/ISF Radiosonde NetCDF Data Files, UCAR/NCAR - Earth Observing Laboratory. https://doi.org/10.5065/D65X27SR.

Wang, J., Bian, J., Brown, W. O., Cole, H., Grubišić, V., and Young, K. (2009). Vertical Air Motion from T-REX Radiosonde and Dropsonde Data, *J. Atmos. Ocean. Technol.*, *26*, 928-942, doi:10.1175/2008JTECHA1240.1